

ADA081653

AFML-TR-78-155

LEVEL

(Handwritten circled 'D')

~~XXXXXXXXXX~~

DTIC
ELECTE
MAR 11 1980
S **D**
C

**COMPLETE FATIGUE CRACK GROWTH RATE CURVES
FOR ALUMINUM ALLOY 2124-T851
INCLUDING TYPICAL CRACK GROWTH MODELS**

*JOHN J. RUSCHAU
UNIVERSITY OF DAYTON RESEARCH INSTITUTE
300 COLLEGE PARK AVENUE
DAYTON, OHIO 45469*

NOVEMBER 1978

TECHNICAL REPORT AFML-TR-78-155
Interim Technical Report May 1976 – May 1978

Approved for public release; distribution unlimited.

AIR FORCE MATERIALS LABORATORY
AIR FORCE WRIGHT AERONAUTICAL LABORATORIES
AIR FORCE SYSTEMS COMMAND
WRIGHT-PATTERSON AIR FORCE BASE, OHIO 45433

80 3 7 061

NOTICE

When Government drawings, specifications, or other data are used for any purpose other than in connection with a definitely related Government procurement operation, the United States Government thereby incurs no responsibility nor any obligation whatsoever; and the fact that the government may have formulated, furnished, or in any way supplied the said drawings, specifications, or other data, is not to be regarded by implication or otherwise as in any manner licensing the holder or any other person or corporation, or conveying any rights or permission to manufacture, use, or sell any patented invention that may in any way be related thereto.

This technical report has been reviewed by the Information Office (ASD/OIP) and is releasable to the National Technical Information Service (NTIS). At NTIS, it will be available to the general public, including foreign nations.

This technical report has been reviewed and is approved for publication.

David C Watson
DAVID C. WATSON
Engineering and Design Data
Materials Integrity Branch

Clayton Harmsworth
CLAYTON HARMSWORTH
Technical Manager
Engineering and Design Data
Materials Integrity Branch

FOR THE COMMANDER:

T. Cooper
TOM COOPER, Chief
Materials Integrity Branch
Systems Support Division
Air Force Materials Laboratory

Copies of this report should not be returned unless return is required by security considerations, contractual obligations, or notice on a specific document.

UNCLASSIFIED

SECURITY CLASSIFICATION OF THIS PAGE (When Data Entered)

19 REPORT DOCUMENTATION PAGE		READ INSTRUCTIONS BEFORE COMPLETING FORM	
1. REPORT NUMBER 18 AFML TR-78-155	2. GOVT ACCESSION NO.	3. RECIPIENT'S CATALOG NUMBER 7	
4. TITLE (and Subtitle) COMPLETE FATIGUE CRACK GROWTH RATE CURVES FOR ALUMINUM ALLOY 2124-T851 INCLUDING TYPICAL CRACK GROWTH MODELS		5. TYPE OF REPORT & PERIOD COVERED Interim Technical Report, May 1976 - May 1978	
6. AUTHOR(S) 10 John J. Ruschau		7. PERFORMING ORG. REPORT NUMBER 14 UDR-TR-78-64	
8. PERFORMING ORGANIZATION NAME AND ADDRESS University of Dayton Research Institute 300 College Park Avenue Dayton, Ohio 45469		9. CONTRACT OR GRANT NUMBER(s) 15 F33615-78-C-5002	
9. PERFORMING ORGANIZATION NAME AND ADDRESS University of Dayton Research Institute 300 College Park Avenue Dayton, Ohio 45469		10. PROGRAM ELEMENT, PROJECT, TASK AREA & WORK UNIT NUMBERS 16 2421 17 03-05	
11. CONTROLLING OFFICE NAME AND ADDRESS		12. REPORT DATE 11 November 1978	
14. MONITORING AGENCY NAME & ADDRESS (if different from Controlling Office) 12 36		13. NUMBER OF PAGES 35	
16. DISTRIBUTION STATEMENT (of this Report) Approved for public release; distribution unlimited.		15. SECURITY CLASS. (of this report) Unclassified	
17. DISTRIBUTION STATEMENT (of the abstract entered in Block 20, if different from Report)		15a. DECLASSIFICATION/DOWNGRADING SCHEDULE	
18. SUPPLEMENTARY NOTES			
19. KEY WORDS (Continue on reverse side if necessary and identify by block number) aluminum fatigue crack growth crack growth models 2124-T851 threshold elongated compact fracture toughness compliance specimen			
20. ABSTRACT (Continue on reverse side if necessary and identify by block number) Complete fatigue crack growth rate curves for aluminum alloy 2124-T851 were developed for two stress ratios: R = +0.1 and +0.5. The data sets obtained range from the threshold stress intensity range, ΔK_{TH} , to the value of stress intensity required for unstable crack propagation. Crack length measurements were obtained using both the traditional visual method and a compliance method developed for the elongated compact specimen. Humidity and			

DD FORM 1 JAN 73 1473

EDITION OF 1 NOV 65 IS OBSOLETE

UNCLASSIFIED

SECURITY CLASSIFICATION OF THIS PAGE (When Data Entered)

10570

1B

UNCLASSIFIED

SECURITY CLASSIFICATION OF THIS PAGE(When Data Entered)

20. Abstract (Concluded)

temperature were controlled and the effect of specimen thickness was examined. For a constant stress intensity range the effect of an increase in R-ratio was to increase the growth rate. The crack growth rate data obtained via the visual and compliance methods are in good agreement over the range investigated. No thickness effect was observed. A variety of model equations were statistically fitted to the data. These models include the Paris, Walker, and Forman equations along with a form of the hyperbolic equation. These equations were examined for accuracy with advantages and shortcomings noted.

UNCLASSIFIED

SECURITY CLASSIFICATION OF THIS PAGE(When Data Entered)

PREFACE

This interim technical report was submitted by the University of Dayton Research Institute, Dayton, Ohio, under contract F33615-78-C-5002, "Quick Reaction Evaluation of Materials," with the Air Force Materials Laboratory, Wright-Patterson Air Force Base, Ohio. This work was initiated under contract F33615-76-C-5034. Mr. David Watson, AFML/MXA, was the Laboratory Project Monitor for this program.

This effort was conducted during the period of May 1976 through May 1978. The author, Mr. John J. Ruschau, was responsible for the direction of the program, and would like to extend recognition to Mr. Eblin of the University of Dayton for performing all testing involved in this reported program. The author would also like to extend special recognition to Dr. Dale Ford of the University of Dayton and Capt. Allen Miller of the Air Force Materials Laboratory for their assistance in the computer programming aspects of this investigation.

This report was submitted by the author in July 1978.

Accession For	
NTIS GRA&I	<input checked="" type="checkbox"/>
DDC TAB	<input type="checkbox"/>
Unannounced	<input type="checkbox"/>
Justification	<input type="checkbox"/>
By _____	
Distribution/	
Availability Codes	
Dist	Avail and/or special
A	

TABLE OF CONTENTS

<u>SECTION</u>		<u>PAGE</u>
I	INTRODUCTION	1
II	MATERIALS AND SPECIMENS	2
III	TEST PROCEDURES	5
IV	RESULTS AND DISCUSSION	8
	REFERENCES	26

LIST OF ILLUSTRATIONS

<u>FIGURE</u>		<u>PAGE</u>
1	Aluminum Alloy 2124-T851 Microstructure Composite (100X)	3
2	Standard Tensile Test Specimen	4
3	Fracture Toughness and Fatigue Crack Growth Specimens	4
4	Constant Amplitude Fatigue Crack Growth Rate Curves for Aluminum Alloy 2124-T851 at R-Ratio of +0.1	10
5	Constant Amplitude Fatigue Crack Growth Rate Curves for Aluminum Alloy 2124-T851 at R-Ratio of +0.5	11
6	Calibration Curve for Elongated Compact Type Specimen	13
7	A Comparison Between Visual and Compliance Methods on Fatigue Crack Growth Rate for a Thickness of 0.75 inch (19.0 mm), R = +0.1	14
8	A Comparison Between Visual and Compliance Methods on Fatigue Crack Growth Rate for a Thickness of 1.5 inch (38.1 mm), R = +0.1	15
9	Photomicrograph of Fatigue Fracture Face of Aluminum 2124-T851, 0.75 inch (19.0 mm) Thick, for $\Delta K = 15.2 \text{ KSI}\sqrt{\text{in}}$ (16.7 MPa $\sqrt{\text{m}}$)	17
10	Photomicrograph of Fracture Face of Aluminum 2124-T851, 1.50 inch (38.1 mm) Thick, for $\Delta K = 15.0 \text{ KSI}\sqrt{\text{in}}$ (16.5 MPa $\sqrt{\text{m}}$)	17
11	A Comparison Between Visual and Compliance Methods on Fatigue Crack Growth Rate for a Thickness of 0.375 inch (9.5 mm), R = +0.5	18
12	Paris Model Equation for Aluminum Alloy 2124-T851 at R-Ratios of +0.1 and +0.5	19
13	Walker Model Equation for Aluminum Alloy 2124-T851	21
14	Forman Model Equation for Aluminum Alloy 2124-T851	23
15	Hyperbolic Sine Model Equation for Aluminum Alloy 2124-T851 at R-Ratios of +0.1 and +0.5	25

LIST OF TABLES

<u>TABLE</u>		<u>PAGE</u>
1	Tensile Properties of Aluminum Alloy 2124-T851 Two-Inch (50.8 mm) Thick Plate	9
2	Fracture Toughness Properties of Aluminum Alloy 2124-T851 Two-Inch (50.8 mm) Thick Plate	9

SUMMARY

The following conclusions are based on test results from a single 2-inch (50.8 mm) thick plate of aluminum alloy 2124-T851. All model equations obtained can be considered accurate only over the ranges specified in this report and should not be extrapolated.

1. The thresholds for constant amplitude fatigue crack growth for this material tested at R-ratios of +0.1 and +0.5 are 2.4 and 1.6 KSI $\sqrt{\text{in}}$ (2.63 and 1.76 MPa $\sqrt{\text{m}}$), respectively.

2. Increasing R-ratio has the effect of increasing the crack growth rate for a given stress intensity range; the threshold stress intensity range decreased with increasing R-ratio.

3. There was no effect of specimen thickness on the fatigue crack growth rate for either R-ratio investigated.

4. No effect of specimen geometry on fatigue crack growth data was observed for the compact type (CT) and the elongated compact type specimen. However, the elongated CT specimens were prone to out-of-plane cracking, while the CT specimens were not.

5. The compliance method for crack length monitoring is a practical and accurate method which lends itself toward a completely automated crack growth data acquisition system. The compliance equation for the elongated CT specimen is in good agreement with the reference compliance equation generated for the CT specimen.

6. The following model equations were obtained for this material undergoing constant amplitude fatigue crack growth testing:

a. Paris Equation

$$\begin{aligned}\frac{da}{dN} &= 1.86 \times 10^{-9} \Delta K^{3.14} @ R = +0.1 \\ &= 2.86 \times 10^{-9} \Delta K^{3.35} @ R = +0.5\end{aligned}$$

b. Walker Equation

$$\frac{da}{dN} = 1.48 \times 10^{-9} [K_{\max}(1-R)^{0.297}]^{3.14}$$

c. Forman Equation

$$\frac{da}{dN} = \frac{1.014 \times 10^{-7} \Delta K^{2.63}}{30.5(1-R) - \Delta K}$$

d. Hyperbolic Sine Equation

$$\log \frac{da}{dN} = 0.97 \sinh (2.92(\log \Delta K - 0.86)) - 5.97 @ R = +0.1$$

$$\log \frac{da}{dN} = 0.97 \sinh (2.88(\log \Delta K - 0.63)) - 6.39 @ R = +0.5$$

SECTION I
INTRODUCTION

Due to the increasing wide usage of aluminum alloy 2124-T851 in present Air Force systems, there currently exists the need to thoroughly document a variety of mechanical properties for this structural material. One important mechanical property of interest for this alloy is its fatigue crack growth rate characteristics. Prior to these results, no consistent data set, produced by a single source, exists that documents the entire da/dN -curve from the threshold up to a growth rate where K_{max} is approaching the critical fracture toughness. Also, due to the ever increasing nondestructive inspecting capabilities, fatigue crack growth rate properties at or near the threshold for crack propagation are becoming of prime concern to the designers and life prediction analysts. It is because of a lack of a consistent data set for 2124-T851 that this program was initiated.

The complete fatigue crack growth rate curves were obtained for aluminum alloy 2124-T851 for two stress ratios. Threshold values of stress intensity range were determined for each stress ratio investigated. The effect of specimen thickness on crack growth properties were examined for both stress ratios. Also, as an aid to future fatigue crack growth investigations, a compliance technique to obtain the necessary test record was developed using the elongated compact type specimen geometry. Finally, a variety of mathematical models currently employed in the technical community were statistically fitted to the data sets and examined.

SECTION II
MATERIALS AND SPECIMENS

The test material used in this investigation was a single 2.0-inch (50.8 mm) thick plate of aluminum alloy 2124-T851. A chemical analysis was performed on the material, yielding the following chemical composition:

CHEMICAL COMPOSITION, % by weight

Cu	Mg	Mn	Si	Fe	Ti	Al
3.9	1.3	0.54	0.08	0.14	<0.03	Balance

These results are within the ranges published by the Aluminum Association^[1] for this material. Photomicrographs illustrating the microstructure in the three principal plate directions are presented in Figure 1.

Tensile specimens were removed from the longitudinal orientation of the test plate and machined to the configuration shown in Figure 2. Two-inch (50.8 mm) thick compact type (CT) fracture toughness specimens were removed from the test plate having longitudinal-transverse orientation (L-T) and machined in accord with Figure 3. Elongated compact type specimens ($H/W = 0.486$) for crack growth investigations were likewise machined from the same orientation (L-T) and machined to the dimensions shown in Figure 3. These specimens were machined in three thicknesses, holding the profile dimensions constant, so the effect of specimen thickness on fatigue crack growth properties could be examined. Because of occasional out-of-plane cracking problems experienced with this specimen geometry during the course of testing, particularly at a stress ratio of $R = +0.5$, the elongated CT specimens were later remachined to the configuration of a CT specimen ($H/W = 0.60$) by reducing the specimen width (W in Figure 3).

[1] Aluminum Standards and Data, The Aluminum Association, 1976.

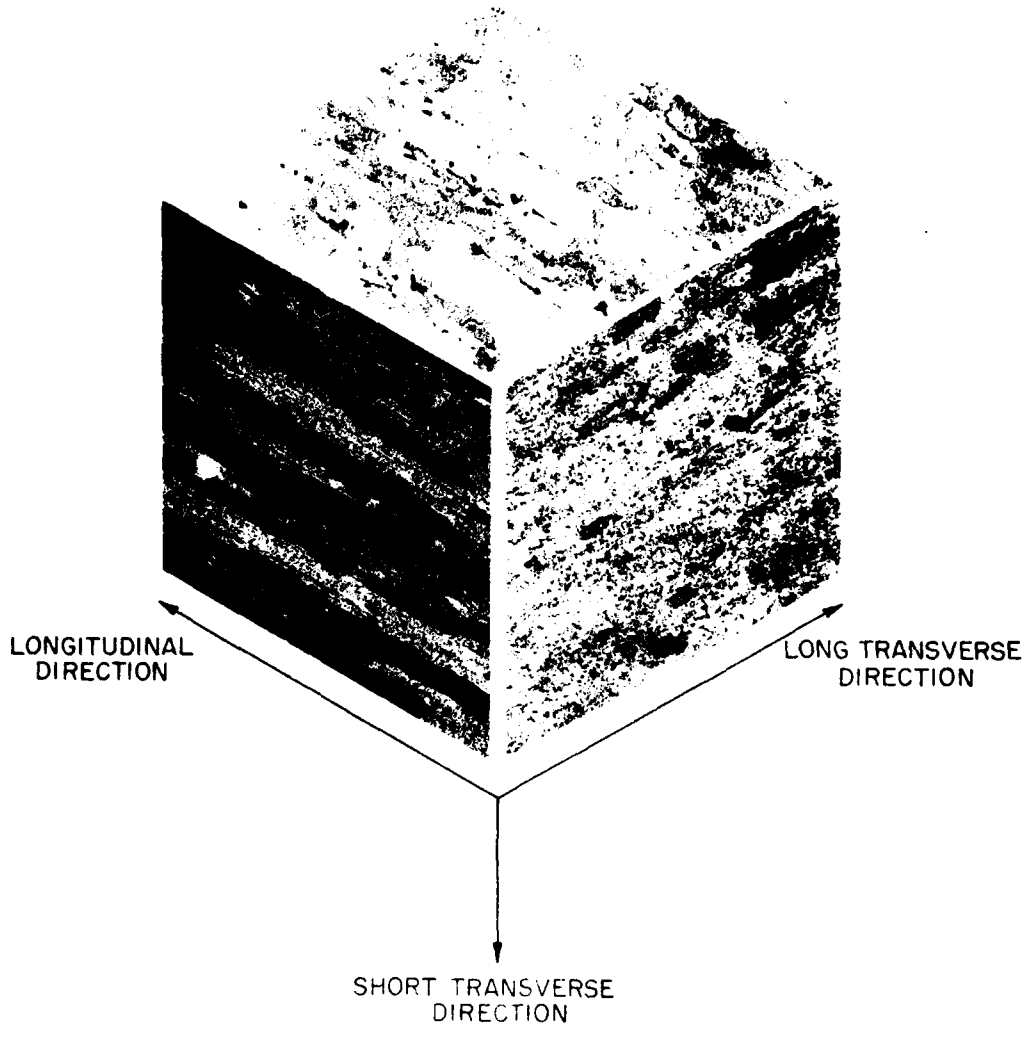


Figure 1. Aluminum Alloy 2124-T851 Microstructure Composite (100X)

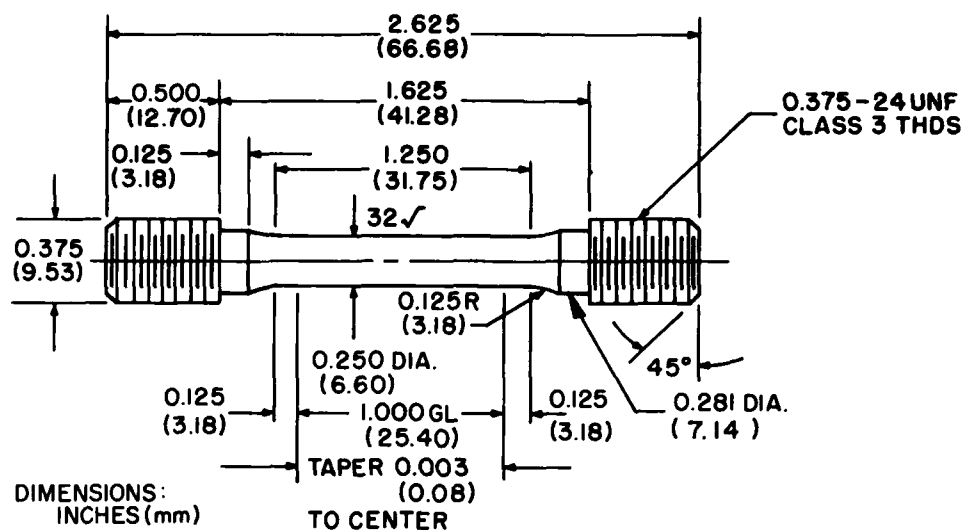
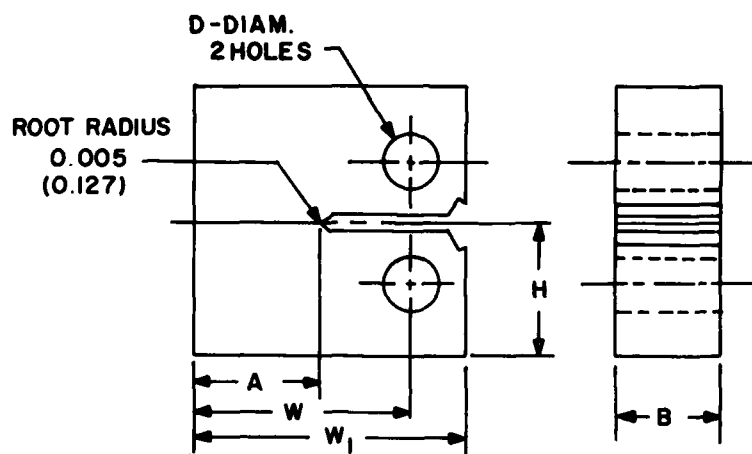


Figure 2. Standard Tensile Test Specimen



DIMENSIONS: INCHES (mm)

SPECIMEN TYPE	A	B	W	W ₁	H	D
FRACTURE TOUGHNESS	2.250 (57.15)	2.000 (50.80)	4.000 (101.60)	4.625 (117.48)	2.400 (60.96)	0.625 (15.87)
CRACK* GROWTH	1.785 (45.3)	0.375 (9.52)	2.550 (64.8)	3.188 (80.9)	1.240 (31.5)	0.500 (12.7)
CRACK* GROWTH	1.785 (45.3)	0.750 (19.05)	2.550 (64.8)	3.188 (80.9)	1.240 (31.5)	0.500 (12.7)
CRACK* GROWTH	1.785 (45.3)	1.500 (38.1)	2.550 (64.8)	3.188 (80.9)	1.240 (31.5)	0.500 (12.7)

* ELONGATED COMPACT SPECIMEN

Figure 3. Fracture Toughness and Fatigue Crack Growth Specimens

SECTION III TEST PROCEDURES

Tensile testing was performed on a Baldwin Wiedemann tensile testing machine. Strain was obtained with a 1.0-inch (25.4 mm) Instron extensometer. Tensile testing was carried out in accordance with ASTM Standard E8-69.

Fracture toughness testing was accomplished using a Tinius-Olsen tensile testing machine following guidelines set forth in ASTM E399-74. Crack opening-displacement (COD) was monitored with a clip-on gage as described in the test standard.

All fatigue crack growth rate testing was carried out with a 2.5 KIP (11.1 kN) MTS hydraulic fatigue testing machine operating in a load-controlled mode. Two stress ratios were employed in this program: $R = +0.1$ and $+0.5$. Test frequency was limited to 30 Hz and all testing was conducted at room temperature. To minimize intralaboratory effects, humidity chambers were fashioned from plexiglass, with humidity limited to less than 10 percent using a dessicant material. Procedures outlined in the proposed standard for constant amplitude fatigue crack growth rate testing^[2] were adhered to as close as possible. The K-Increasing Constant-Amplitude-Load Control method was employed for all specimens. Two methods were employed to gather the necessary test data and are outlined in the following paragraphs. Crack growth rates obtained from each method were finally compared to striation spacings measured from photomicrographs taken of the fracture faces.

The first method, widely used by the majority of testing laboratories and thoroughly described in the proposed standard for crack growth testing, employed a 30X traveling microscope to measure the fatigue crack length on each surface of the specimen. After a predetermined number of load cycles [sufficient to yield an estimated crack extension of 0.010 to 0.020 inch (0.25 to 0.50 mm)] the test machine was halted, a mean load applied to

[2] Hudak, S.J., et al., Development of Standard Methods of Testing and Analyzing Fatigue Crack Growth Rate Data, AFML-TR-78-40, 1978.

enhance the fatigue crack tip, and a visual measurement of crack length taken, after which the testing machine was restarted. This procedure was continued until complete specimen fracture. A crack curvature correction factor was determined using the same guidelines for crack length correction set forth in ASTM 399 for Fracture Toughness Testing. This correction was added to each visual trace previously taken, along with the length of the starter notch (from centerline of loading holes to notch tip) to obtain the raw crack growth data set of crack length "a", and corresponding number of load cycles, "N". These data were then reduced to the standard accepted form (crack growth rate, da/dN , as a function of change in stress intensity, ΔK) in the manner prescribed in the aforementioned proposed test standard. This method fits a second-order polynomial to a seven-point data subset, and in turn calculates the slope at the midpoint of the subset. The midpoint crack length is used to calculate the ΔK value, while the slope is the corresponding da/dN value. This procedure is applied throughout the entire raw data set to generate the da/dN vs. ΔK curve.

While the previously described testing procedures were being applied, fatigue crack length measurements were simultaneously being recorded in a different fashion using a compliance technique which relates crack length as a function of crack opening-displacement. Hardened steel knife edges were affixed to the specimen and an MTS clip gage used to monitor specimen COD. Displacement was measured at a distance 0.125 inch (3.18 mm) from the front surface of the specimen. The signal from the clip gage was fed to an X-Y recorder; COD to the X-axis, load to the Y-axis. Each time the cyclic loading was halted for a visual crack length measurement, a trace of specimen COD vs. load was recorded. To obtain this, the load was slowly applied to approximately 90 percent of the maximum cyclic load. After completing this trace, fatigue loading was resumed and the same procedures applied after crack extension of approximately 0.010 inch (0.254 mm). Values of crack length

were then calculated from the slopes of the COD vs. load curves using the necessary compliance equation. Crack growth rate data were obtained from these data, using the same computation routines used to reduce the visually obtained data.

The compliance curve was generated using two specimen thicknesses: 0.375 inch (9.52 mm) and 0.75 inch (19.0 mm). This procedure involved precracking ($R = +0.1$) to a certain crack length an elongated compact type specimen instrumented with the clip gage. Load was then applied slowly and a trace of load vs. COD was obtained with an X-Y recorder. The specimen was then further fatigue cracked to a different crack length and the same technique repeated. Again, at the conclusion of the routine, the specimen was broken apart and a curvature correction factor carefully obtained and added to each visual reading. A series of curves was obtained for the $\frac{a}{w}$ (crack length/specimen width) range of 0.35 to 0.65. Normalized values of crack-opening-displacement and crack length were then plotted and an expression developed relating the specimen COD to crack length.

Upon the generation of the entire crack growth rate curves, a variety of mathematical models, developed to describe the constant amplitude crack growth relationship, were statistically fitted to the data and compared for best fit. Models investigated were the Paris Power Law equation, the Walker equation, the Forman equation, and a form of the hyperbolic sine equation. [3] A computer program, listed in the computer library at Wright-Patterson Air Force Base (WPAFB) as SIMPLEX, was used to fit the data. This program fits any given form of an equation to a furnished data set. The program utilizes a least squares regression technique to determine the unknown constants and also computes a maximum and standard deviation for checking accuracy of fit. In order to treat all portions of the data set with equal weight, logarithmic values of da/dN and ΔK were analyzed. The resulting equations were then transposed back to the

[3] Annis, C.G., Jr., et al., An Interpolative Model for Elevated Temperature Fatigue Crack Propagation, AFML-TR-76-176, November 1976.

nonlogarithmic form, with the exception of the hyperbolic sine equation which was left as $\log da/dN$ as a function of $\log \Delta K$.

SECTION IV RESULTS AND DISCUSSION

The tensile test results for specimens tested in the longitudinal orientation are presented in Table 1 and are in good agreement with published data. [4,5] Fracture toughness test results for longitudinal-transverse oriented specimens are listed in Table 2 and are also in agreement with References [4] and [5].

The fatigue crack growth rate curves for aluminum alloy 2124-T851 for R-ratios of +0.1 and +0.5 are presented in Figures 4 and 5, respectively. The curves presented in both figures represent data obtained from 16 specimens per R-ratio. The threshold value of stress intensity range, ΔK_{TH} , for R = +0.1 testing is approximately $2.4 \text{ KSI}\sqrt{\text{in}}$ ($2.63 \text{ MPa}\sqrt{\text{m}}$); the threshold stress intensity range for R = +0.5 testing is approximately $1.6 \text{ KSI}\sqrt{\text{in}}$ ($1.76 \text{ MPa}\sqrt{\text{m}}$). The curves obtained for both R-ratios demonstrate unstable crack propagation occurring when K_{max} is approximately $30 \text{ KSI}\sqrt{\text{in}}$ ($33 \text{ MPa}\sqrt{\text{m}}$), which coincidentally is the critical fracture toughness, K_{IC} , for this material.

The effect of specimen thickness on fatigue crack growth was examined only at growth rates above 10^{-6} in/cyc. (25.4 nm/cyc.) since it was felt it would be more difficult to maintain a symmetric crack front at low ΔK values for the thicker specimens. For the three thicknesses investigated there does not appear to be any thickness effect on crack growth rates below

[4] Fudge, K.A. and Jones, R.E., Engineering Design Data for Aluminum Alloy 2124-T851 Thick Plate, AFML-TR-73-310, January 1974.

[5] Cervay, R.R., Temperature Effects on the Mechanical Properties of Aluminum Alloy 2124-T851, AFML-TR-75-208, December 1975.

TABLE 1
TENSILE PROPERTIES OF ALUMINUM ALLOY
2124-T851 TWO-INCH (50.8 mm) THICK PLATE

Specimen No.	Yield Strength KSI (MPa)	Ultimate Strength KSI (MPa)	% Elongation in 1.0 inch (25.4 mm) Gage Length	Reduction in Area (%)
X1	65.6 (452)	71.9 (496)	9.0	21.5
X2	67.0 (462)	72.5 (500)	9.1	22.6
X3	<u>66.7 (460)</u>	<u>71.9 (496)</u>	<u>9.0</u>	<u>21.2</u>
Avg.	66.4 (458)	72.1 (497)	9.0	21.7

TABLE 2
FRACTURE TOUGHNESS PROPERTIES OF ALUMINUM ALLOY
2124-T851 TWO-INCH (50.8 mm) THICK PLATE

Specimen No.	Orientation	K_{IC} KSI $\sqrt{\text{in}}$	(MPa $\sqrt{\text{m}}$)
1C	Long.-Transverse	30.1	(33.1)
2C	Long.-Transverse	30.9	(34.0)
3C	Long.-Transverse	<u>30.4</u>	<u>(33.4)</u>
Avg.		30.5	(33.5)

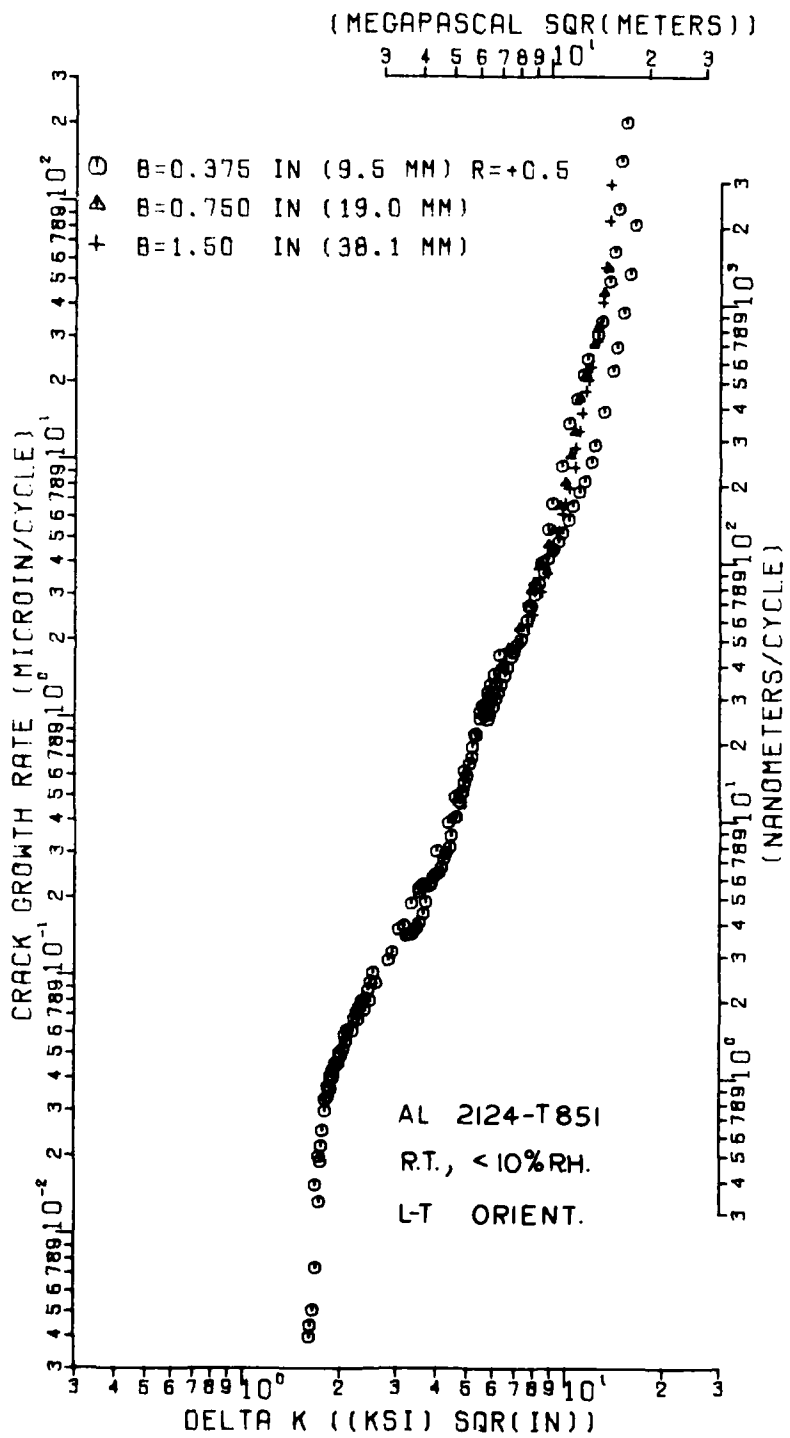


Figure 5. Constant Amplitude Fatigue Crack Growth Rate Curves for Aluminum Alloy 2124-T851 at R-Ratio of +0.5

10^{-4} in/cyc. (2.5×10^3 nm/cyc.). This fact is in good agreement with the findings of Reference [2] where it was noted that any apparent variation in fatigue crack growth rate data due to thickness results from inaccuracies in the crack length measurements due to nonsymmetric crack front curvature or tunneling.

Crack Length Determination via Compliance Method

Normalized values of crack length with corresponding normalized values of crack opening-displacement were obtained for a number of elongated compact type specimens of various thicknesses. A third-degree polynomial was fitted to the data yielding the following expression:

$$\frac{E \cdot B \cdot \text{COD}}{P} = -348.6 + 2492 \left(\frac{a}{w}\right) - 5512 \left(\frac{a}{w}\right)^2 + 4431 \left(\frac{a}{w}\right)^3$$

or

$$\begin{aligned} \frac{a}{w} = & 0.0677 + 0.00894 \left(\frac{E \cdot B \cdot \text{COD}}{P}\right) - 0.000049 \left(\frac{E \cdot B \cdot \text{COD}}{P}\right)^2 \\ & + 0.00000101 \left(\frac{E \cdot B \cdot \text{COD}}{P}\right)^3 \end{aligned}$$

where E is the material's modulus of elasticity, B is the specimen thickness, COD is the displacement as measured by the clip gage, and P is the applied load.

The first equation is illustrated in the computer-prepared curve shown in Figure 6 along with a similar curve [6] developed from aluminum alloys 7075-T6 and 2024-T351, titanium 6Al-4V, and 4340 steel using a CT specimen geometry of equal overall width (W_1 in Figure 3). Deviation between the two curves is small over the range of $\frac{a}{w}$ from 0.35 to 0.60. For crack length/width ratios above this, differences between the two curves become greater with increasing values of $\frac{a}{w}$.

Crack growth rate data obtained employing the visual method are presented in Figures 7 and 8 for a stress ratio of $R = +0.1$

[6] Sullivan, A.M., Crack Length Determination for the Compact Tension Specimen Using a Crack-Opening Displacement Calibration, NRL Report 7888, June 1975.

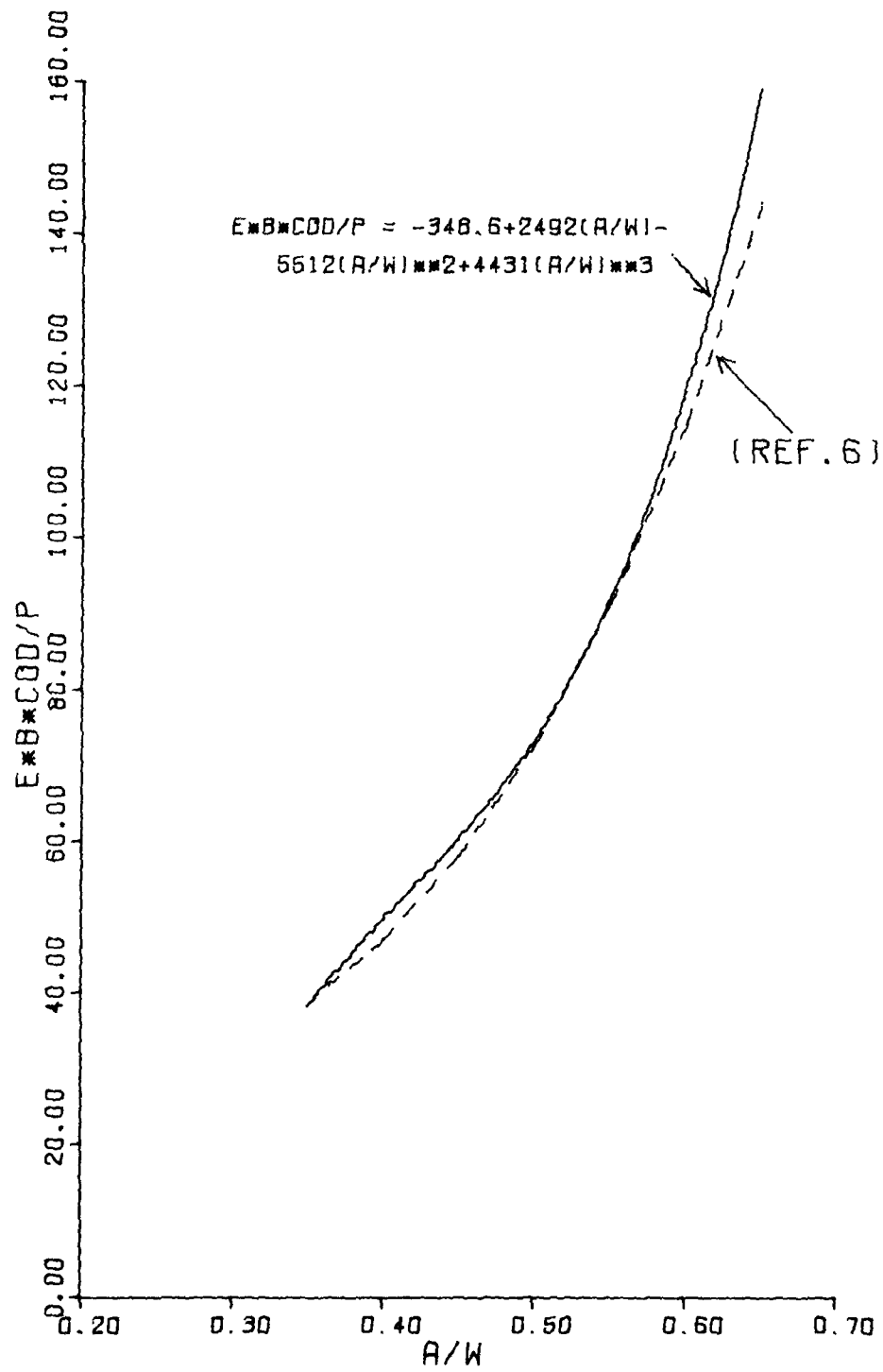


Figure 6. Calibration Curve for Elongated Compact Type Specimen

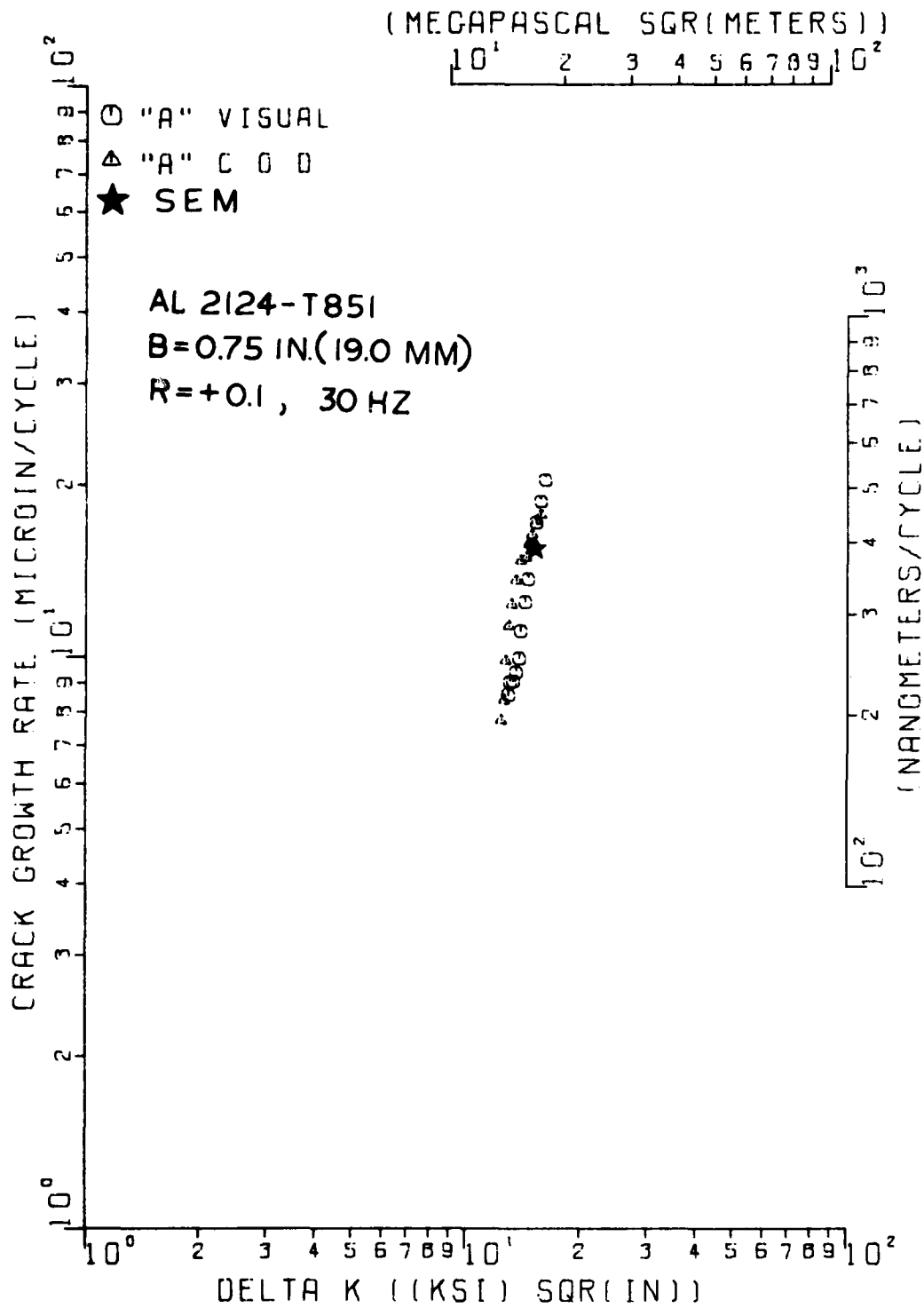


Figure 7. A Comparison Between Visual and Compliance Methods on Fatigue Crack Growth Rate for a Thickness of 0.75 inch (19.0 mm), R = +0.1

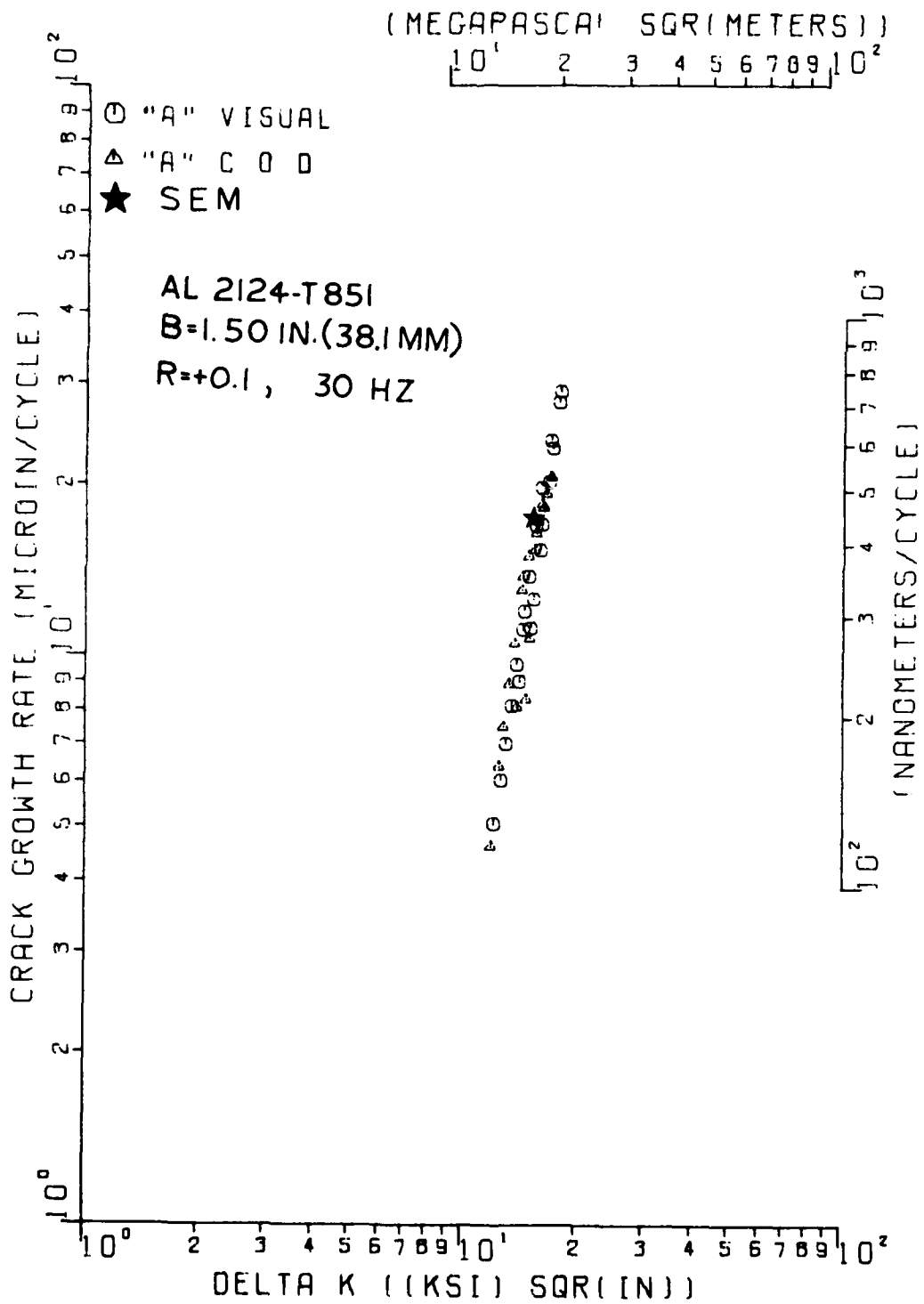


Figure 8. A Comparison Between Visual and Compliance Methods on Fatigue Crack Growth Rate for a Thickness of 1.5 inch (38.1 mm), R = +0.1

along with the crack growth rate data obtained using the compliance (COD) technique. For both thicknesses investigated, the results are identical over the range tested. Photomicrographs obtained with the scanning electron microscope (SEM) for both thicknesses at a stress intensity of approximately $15 \text{ KSI}\sqrt{\text{in}}$ ($16.5 \text{ MPa}\sqrt{\text{m}}$) are presented in Figures 9 and 10. Measurements of the striation spacing on these photographs, which indicate the growth per cycle, are also presented in Figures 7 and 8, verifying both procedures as accurate methods. Compliance technique developed test results for a stress ratio of $R = +0.5$ are similarly presented in Figure 11, along with the "visual" results, for specimen thickness of 0.375 inch (9.50 mm). Again, the results for the compliance method are in excellent agreement with those obtained via the visual method. Because of a poor fracture face topography for this particular sample, a microscopic investigation could not be accomplished.

Fatigue Crack Growth Models

A number of constant amplitude fatigue crack growth rate model equations were statistically fitted to the data obtained from the 0.375-inch (9.52 mm) thick specimens. The most familiar is the Paris Power Law equation, illustrated in Figure 12. This equation, which appears as a straight line on log-log axis, was developed to model the linear portion of the sigmoidal-shaped da/dN vs. ΔK curve. The curves illustrated in Figure 12 were fitted to the test data at R-ratios above both 10^{-7} in/cyc. (2.5 nm/cyc.) and below 10^{-5} in/cyc. (254 nm/cyc.). Crack growth rates are in terms of inches per cycle, while stress intensity range is in $\text{KSI}\sqrt{\text{in}}$.

The Paris equation has the definite advantage of being a compact yet accurate model when considering only the linear portion of the crack growth rate curve; however, it does have limitations. One major shortcoming of this equation is that by making it short and concise, it contains no expression to account for such parameters as varying R-ratios. Consequently,

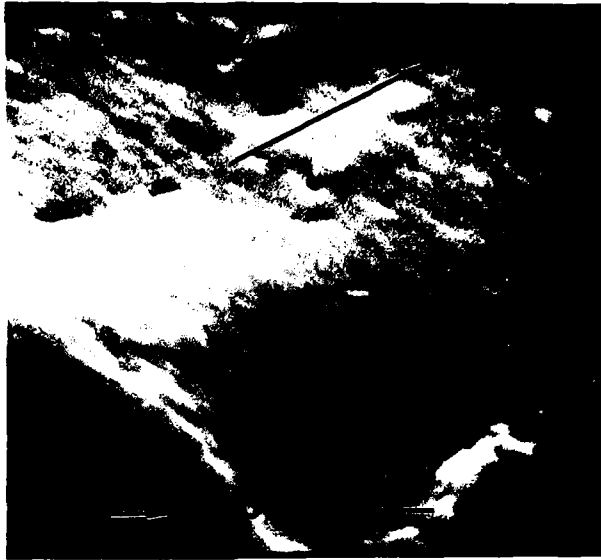


Figure 9. Photomicrograph of Fatigue Fracture Face of Aluminum 2124-T851, 0.75 inch (19.0 mm) Thick, for $\Delta K = 15.2 \text{ KSI}\sqrt{\text{in}}$ ($16.7 \text{ MPa}\sqrt{\text{m}}$)

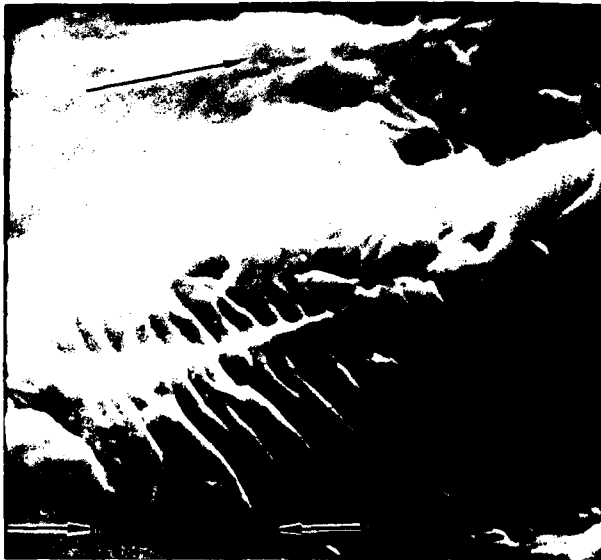


Figure 10. Photomicrograph of Fracture Face of Aluminum 2124-T851, 1.50 inch (38.1 mm) Thick, for $\Delta K = 15.0 \text{ KSI}\sqrt{\text{in}}$ ($16.5 \text{ MPa}\sqrt{\text{m}}$)

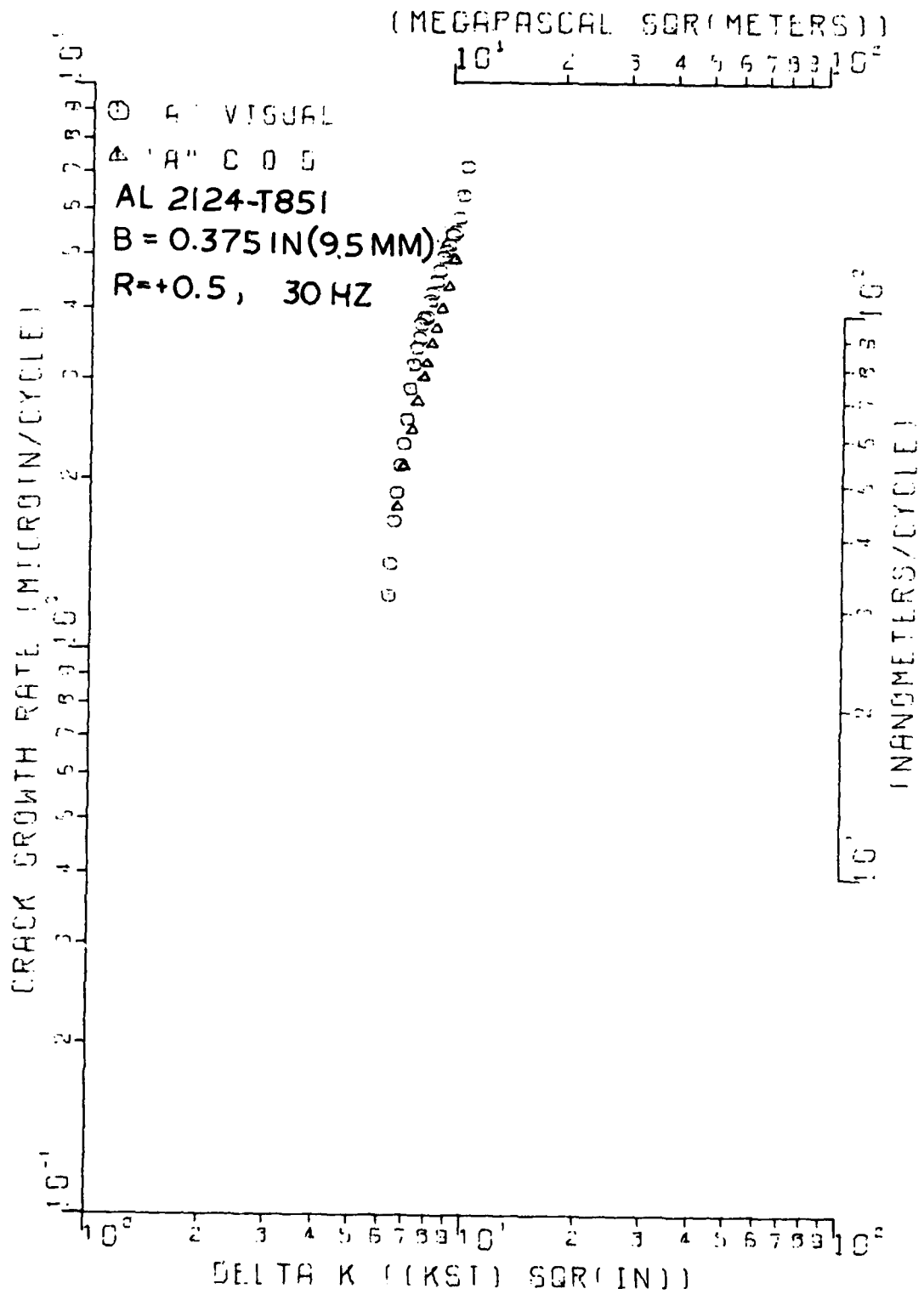


Figure 11. A Comparison Between Visual and Compliance Methods on Fatigue Crack Growth Rate for a Thickness of 0.375 inch (9.5 mm), R = +0.5

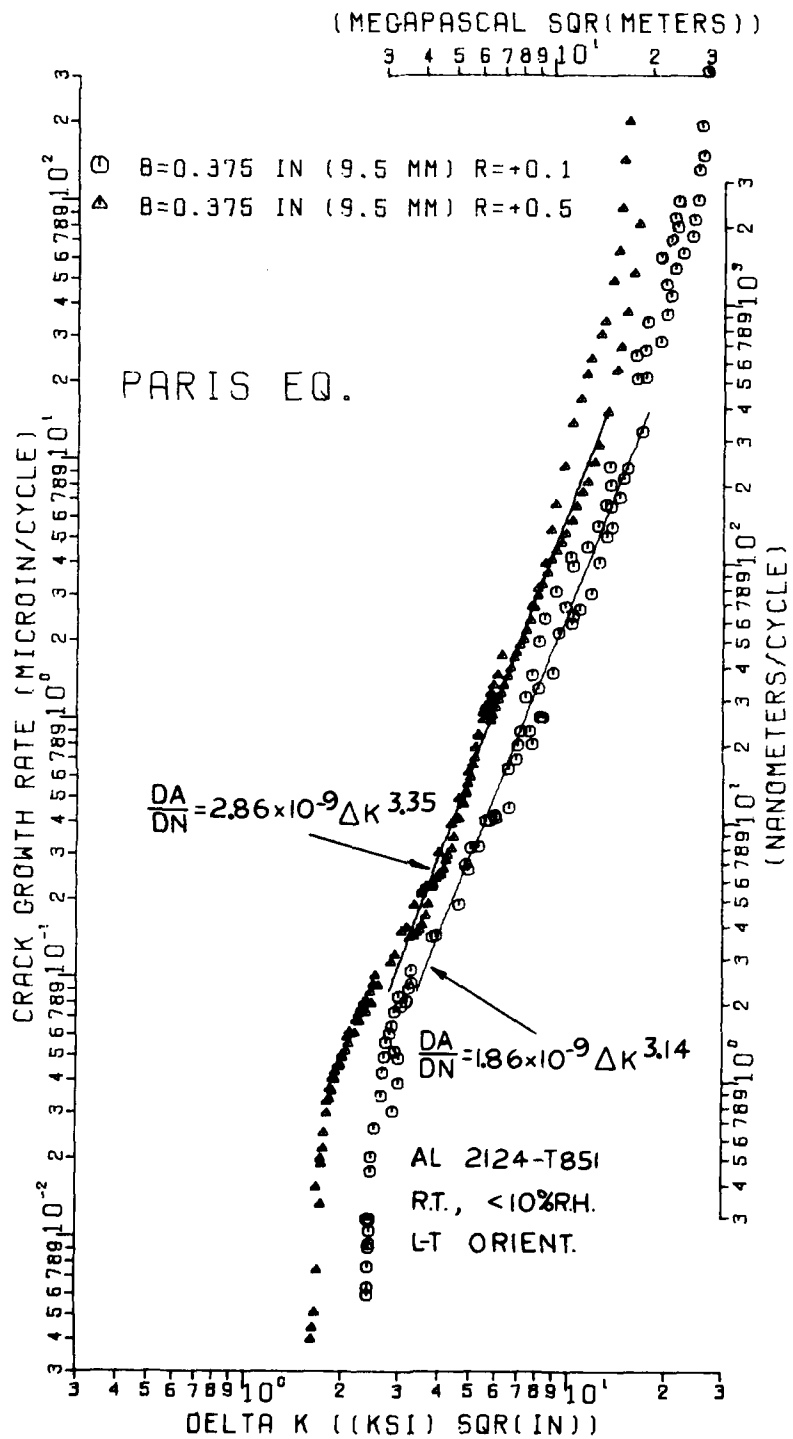


Figure 12. Paris Model Equation for Aluminum Alloy 2124-T851 at R-Ratios of +0.1 and +0.5

different parameters must be used for each different possible R-ratio.

Walker, [7] in his investigation of stress ratio effects on fatigue crack propagation, developed an expression for an effective stress (\bar{S}):

$$\bar{S} = S_{\max} (1-R)^m$$

where S_{\max} is the maximum cyclic stress, and m is an empirically determined constant. This effective stress concept was used to develop an effective stress intensity which, when substituted in the Paris equation, yielded the following equation:

$$da/dN = C(K_{\max}(1-R)^m)^p$$

where K_{\max} is the maximum cyclic stress intensity, and C , p , and m are the empirically derived constants. This equation was fitted to the data developed from the 0.375-inch (9.52 mm) thick specimens used at $R = +0.1$ yielding the following expression:

$$da/dN = 1.483 \times 10^{-9} [K_{\max}(1-R)^{0.297}]^{3.14}$$

where da/dN is again in terms of inches/cycle and K_{\max} is in terms of $KSI\sqrt{in}$. Again data were limited to greater than 10^{-7} in/cyc. (2.5 nm/cyc.) and less than 10^{-5} in/cyc. (254 nm/cyc.). Note that when $R = +0.1$ the equation is identical to the Paris equation previously obtained. This equation is graphically depicted in Figure 13 for R-ratios of +0.1 and +0.5. The Walker model handles the curve shift due to different R-ratios reasonably well as exemplified in the figure.

The Walker equation is more versatile than the Paris equation since only the one equation is needed to define the crack growth rate curve at any stress ratio; however, like the Paris equation, it is applicable only to the linear portion of the da/dN vs. ΔK curve. It does not account for either the

[7] Walker, K., "The Effect of Stress Ratio During Crack Propagation and Fatigue for 2024-T3 and 7075-T6 Aluminum," ASTM STP 426, 1970.

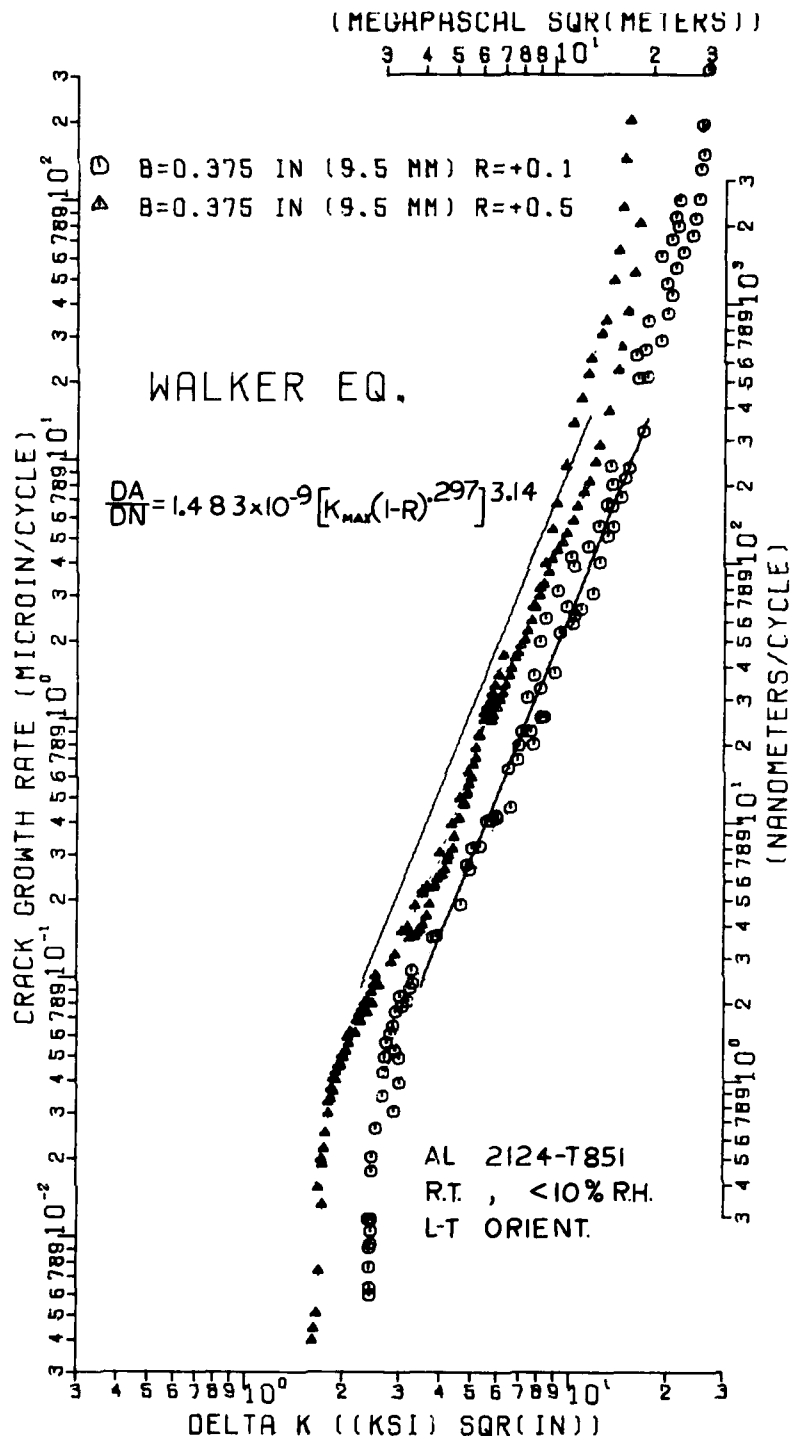


Figure 13. Walker Model Equation for Aluminum Alloy 2124-T851

upper or lower portions of the curve and therefore can lead to large errors if extrapolated beyond its limits.

Forman, et al. [8] developed an expression to handle the acceleration of fatigue crack growth at high stress intensity values for any stress ratio, which has the form

2

$$da/dN = \frac{C\Delta K^P}{(1-R)K_C - \Delta K}$$

where the numerator is simply the Paris equation and K_C is the maximum fracture toughness value at the onset of unstable crack propagation, determined from the vertical asymptote at the upper portion of the da/dN vs. ΔK curve. This equation was fitted to the $R = +0.1$ data (above 10^{-7} in/cyc. [2.5 nm/cyc.]) and is presented in Figure 14 for both R -ratios (+0.1 and +0.5) for a value of K_C of $30.5 \text{ KSI}\sqrt{\text{in}}$ ($33.5 \text{ MPa}\sqrt{\text{m}}$). In addition to handling well the R -ratio shift, the Forman equation accurately models the upper portion as well as the linear portion of the crack growth rate curve. However, as in the case of the two previously mentioned models, it fails to model crack growth rates near the threshold.

A number of investigators have looked at the hyperbolic trigonometric functions as a possible choice for a model since both the hyperbolic sine (\sinh) and hyperbolic tangent (\tanh) expressions yield a sigmoidally-shaped curve. Annis, et al. [3] developed a hyperbolic sine model of the form:

$$\log(da/dN) = C_1 \sinh(C_2(\log(\Delta K) + C_3)) + C_4,$$

where the coefficients are functions of test frequency, stress ratio, and temperature. This expression was fitted to both data sets and the coefficients were statistically determined via the regression technique used for the previously mentioned models. The value C_1 , which controls the vertical "stretch" of the S-shaped

[8] Forman, R.G., et al., "Numerical Analysis of Crack Propagation in Cyclically Loaded Structures," J. of Basic Eng., Trans. ASME, Vol. 89, Series D, September 1967.

curve, is reported to be a fixed value for a given material. For IN-100 material, C_1 has a value of 0.5,^[3] while limited experience with titanium indicated a value of 0.9 yields the best curve.^[9] For this investigation C_1 was varied between 0.5 and 1.5, with results indicating a value of C_1 equal to 0.97 produces the best fit. The results of this analysis are presented in Figure 15. Each curve adequately represents its respective data set throughout the entire da/dN range. The effect of R-ratio is seen as a shift of the curve to the left and slightly down for increasing R-ratio. This same trend was noted by Annis, et al. for IN-100 material tested at various R-ratios.

[9] Corbly, D.M., Air Force Materials Laboratory, Wright-Patterson Air Force Base, Ohio, Personal Communication to John J. Ruschau, July 1978.

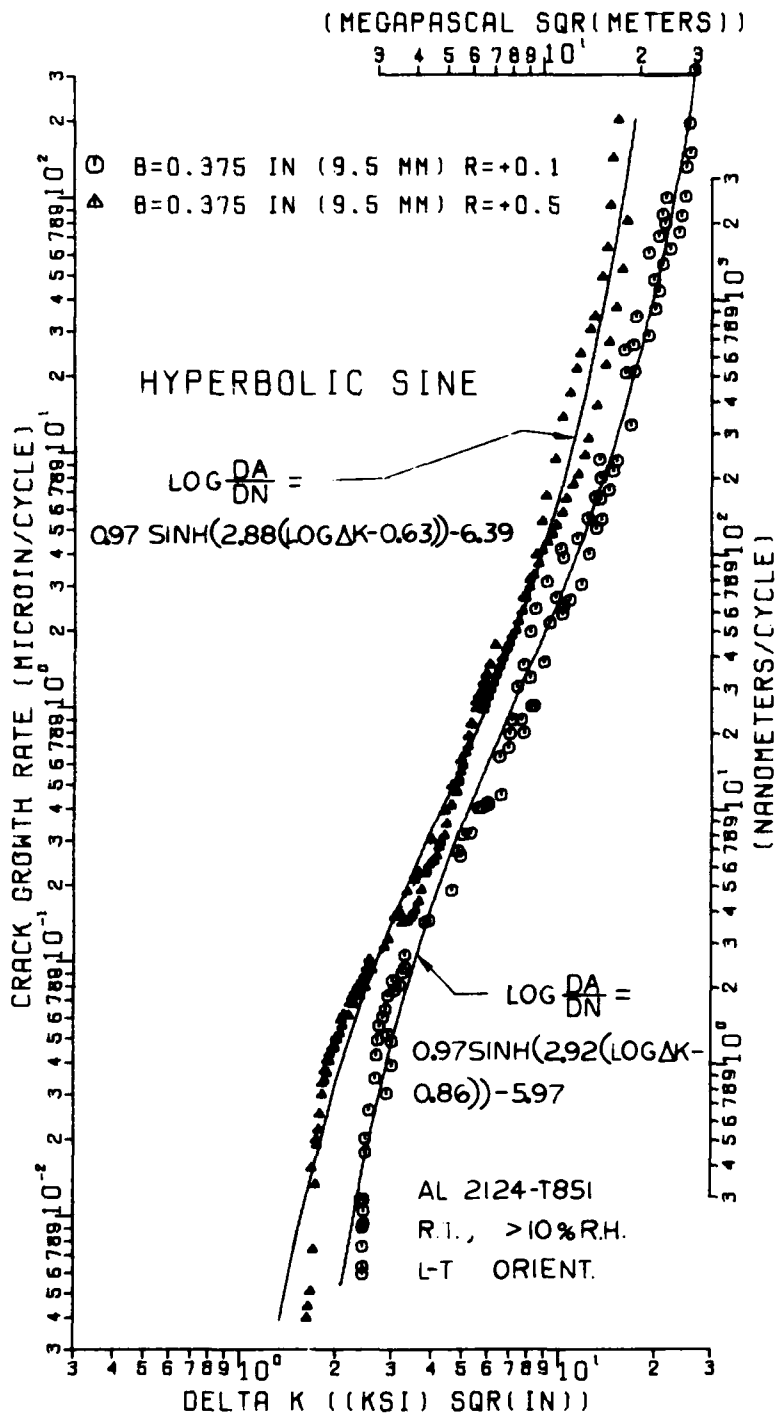


Figure 15. Hyperbolic Sine Model Equation for Aluminum Alloy 2124-T851 at R-Ratios of +0.1 and +0.5

REFERENCES

1. Aluminum Standards and Data, The Aluminum Association, 1976.
2. Hudak, S.J., et al., Development of Standard Methods of Testing and Analyzing Fatigue Crack Growth Rate Data, AFML-TR-78-40, 1978.
3. Annis, C.G., Jr., et al., An Interpolative Model for Elevated Temperature Fatigue Crack Propagation, AFML-TR-76-176, November 1976.
4. Fudge, K.A. and Jones, R.E., Engineering Design Data for Aluminum Alloy 2124-T851 Thick Plate, AFML-TR-73-310, January 1974.
5. Cervay, R.R., Temperature Effects on the Mechanical Properties of Aluminum Alloy 2124-T851, AFML-TR-75-208, December 1975.
6. Sullivan, A.M., Crack Length Determination for the Compact Tension Specimen Using a Crack-Opening Displacement Calibration, NRL Report 7888, June 1975.
7. Walker, K., "The Effect of Stress Ratio During Crack Propagation and Fatigue for 2024-T3 and 7075-T6 Aluminum," ASTM STP 426, 1970.
8. Forman, R.G., et al., "Numerical Analysis of Crack Propagation in Cyclically Loaded Structures," J. of Basic Eng., Trans. ASME, Vol. 89, Series D, September 1967.
9. Corbly, D.M., Air Force Materials Laboratory, Wright-Patterson Air Force Base, Ohio, Personal Communication to John J. Ruschau, July 1978.